Jinst

Published by IOP Publishing for Sissa Medialab

Received: *April 26, 2019*
Revised: *July 18, 2019*
Accepted: *December 12, 2019*
Published: *January 16, 2020*

2020 JINST 15 P01016

Microwave source with enhanced radiation power based on orbitron MASERs

A.H. Esmaeili,[a,b] **S. Matlou,**[b,1] **A. Rostam**[b] **and K. Goudarzi**[a,b]

[a] *Quantum Photonics Research Lab., Faculty of Electrical and Computer Engineering, University of Tabriz, Tabriz, Iran*

[b] *Photonics and Nano-Crystals Research Lab., Faculty of Electrical and Computer Engineering, University of Tabriz, Tabriz, Iran*

E-mail: matloub@tabrizu.ac.ir

Abstract: We have proposed the design of high power microwave source in a vacuum tube based on the theory of negative mass instability. The proposed source does not operate based on a slow-wave structure but instead makes use of accelerated charged particles. In our structure, an electron emitter injects the charged particles into to the cavity. Emitted particles move around the anode, which leads to electron acceleration and emission of electromagnetic waves with a specific frequency. In this paper, we have enhanced the output power and frequency of microwave source by variation of particles initial energy and the number of anodes incorporating their specific arrangement and applied voltages. Working at room temperature, compactness, wide bandwidth, and tunability of output frequency are among the advantages of the proposed source.

Keywords: Accelerator modelling and simulations (multi-particle dynamics; single-particle dynamics); Instrumentation for particle accelerators and storage rings - low energy (linear accelerators, cyclotrons, electrostatic accelerators)

[1]Corresponding author.

https://doi.org/10.1088/1748-0221/15/01/P01016

Contents

2020 JINST 15 P01016

1 Introduction

Electromagnetic radiation sources are of great importance in microwave applications due to their various advantages such as wide bandwidth, prominent directivity, small antennas, and consequently low power consumption. So, the generation of microwaves has been the subject of current studies in various applications such as nondestructive testing [1, 2], radars [3], space [4], sensing [5], communications [6], and point to point communications [7]. Based on these applications, the microwave source with a tunable frequency and high power output is very crucial. Microwave sources in vacuum tubes such as Orbitron MASERs, Gyrotron, Klystron, and Magnetron working based on accelerated electrons have higher output power and efficiency in comparison with solid-state sources such as TUNNEL, IMPATT, and Gunn diodes [8–12]. The microwave vacuum tubes are categorized into slow- and fast-wave tubes. The slow-wave tubes suffer from their need for some specific circuits to decrease microwave phase velocity below the light velocity; this is required to match phase velocity with that of electron's, and is challenging in very high frequency sources due to the direct relationship between their circuit size and the wavelength [10, 13]. Furthermore, these vacuum sources have problems such as their limited radiated frequency, complex structures, and need to relativistic electrons, external magnetic fields, and expensive and enormous equipments.

The Orbitron MASER, as fast-wave device independent of slow-wave systems, can play the role of a microwave radiation source [14]. It radiates based on a physical mechanism known as Negative Mass Instability (NMI) theory similar to Gyrotrons. The electron emitter injects electrons into the tube; due to their angular momentum, they orbit around the central wire in the emitter, and generate the electromagnetic radiation as they lose energy. So, the device can emit high power and tunable frequency radiation in 1GHz-1THz range, which makes it as a suitable candidate for radars and many other applications [12, 15].

The Orbitron MASER consists of a metallic cylinder as the tube in which a wire is positioned closely to the inner shell along the axis of cylinder; this wire plays the role of an electron emitter that injects electrons into the tube. One or more wires, called anodes, are located in the center of the tube. They are connected to specific voltages and responsible for radial electric field distribution inside the tube. Emitted electrons move around anodes, leading to the emission of electromagnetic radiation as a result of their acceleration [15–19]. The extracted mathematical expressions indicate

that this emitter is working based on the theory of NMI theory. NMI theory causes phase bunching of the rotating electrons, which results in coherent microwave emission. The radiation frequency of such a coaxial system depends on the cylinder and anode diameters, the anode voltage, and injected electron density. This Orbitron MASER has highlighted features such as very simple and cost-effective structure, compactness, light weight, high power radiation at pulsed mode, tunable frequency, and ulrtabroadband (GHz-THz) output [14–23]. This emitter can be also applied as an ion source [24] or the gas-filled pulsed device [25, 26]. Other potential applications of this Orbitron MASER include RF waves generation, rugged and battery-powered millimeter-wave radars [12], speed control radars, and nondestructive testing.

The proposed structure can operate in both pulsed and steady-state modes. Both modes have a similar mechanism; i.e., any power or frequency improvement in a steady-state Orbitron can be implemented in the pulse mode [20, 22]. The output power of 10 μW almost at 1GHz frequency with an efficiency less than 0.01% has been reported in a single-anode Orbitron MASER [18]. Also, 1mW radiation power at nearly 1GHz has been observed in a multi-anode system [19, 22]. Our aim in this work is to enhance the output power, frequency and efficiency of the emitted radiation in single frequency condition. To this end, the number of anodes has been increased. Besides, the optimum distance between wires, their voltage difference and arrangement have been investigated. Hence, CST particle studio software package and 3D simulations has been incorporated to simultaneously solve and analyze coupled Maxwell (for electromagnetic section) and Lorentz equations (for electrons and their governing forces).

It is good to be mentioned that the multi-anode Orbitron MASER has been designed and simulated for the first time. Moreover, the multi-anode arrangement with anodes of different voltages have been exploited to increase radiation frequency and power of the MASER; this will lead to more acceleration of the electrons and better phase locking compared to its counterparts with anodes of same voltages. Consequently, high power radiation has been obtained according to the simulation results of this paper. Finally, quasi-single-frequency and power radiation has been observed due to the special proposed design and manipulation of the initial energy for electrons.

The rest of the paper is organized as follows: the theory behind the oscillation frequency of electrons are briefly explained in section 2. The obtained output radiation of electromagnetic waves are described in section 3. This radiation is collected by the port located at the top and bottom of the tube. Additionally, the distribution of electric field and particle valocity for the proposed structure are investigated. The dependence of output power on the anodes spacing for various potential differences is also studied. Finally, section 4 concludes the paper.

2 Theory of orbitron MASER

The Orbitron MASER generates electromagnetic radiation for which the frequency varies in GHz-THz range. The device contains a metal tube working in hard vacuum based on a simple physical mechanism. Due to the lack of need for slow-wave structure, this device is categorized as a fast-wave device capable of generating coherent waves with high output power. It can be built on small scale, which is a considered a significant advantage for vacuum state sources. As NMI theory indicates, rotating particles of different angular velocities can cause phase bunching in these structures. The bunched particles will rotate around the anode wire and radiate coherent electromagnetic waves.

2020 JINST 15 P01016

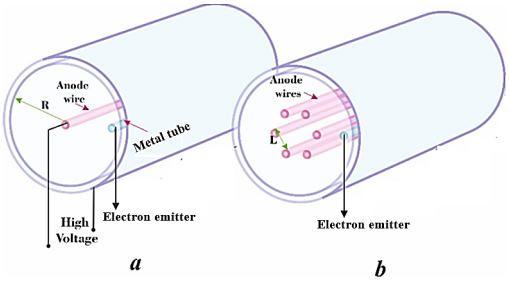

Figure 1. The structure of (a) single anode, (b) multi-anode Orbitron MASER.

As a result of interaction between charged particles themselves and also with the electric field, micro-bunches of different energies are created. Consequently, these micro-bunched electrons lose and gain angular energy, and can respectively move to lower or higher orbits; these clumps (micro-bunched electrons) will have higher angular velocities when losing energy and vice versa [18–20, 22]. So, the broadband radiation of electromagnetic waves at a frequency range of 1GHz-1THz by different angular velocities (or energies) is achievable [15].

Gyrotron is another vacuum tube microwave source based on NMI with a mechanism similar to that of Orbitron MASER. However, there are some crucial differences. As mentioned earlier, injected electrons in Orbitron MASER are electrostatically confined in a potential well and move around the central anode as a result of a natural population inversion; the inversion is caused by loss of some electrons from the system due to the wire potential. Additionally, the Orbitron MASER naturally works based on negative mass theory which necessitates the kinetic energy of electrons to be low. In contrast to this, NMI in Gyrotron requires relativistic energy to achieve population inversion [19, 27]. Another difference is the oscillation of electrons. By interaction with a constant magnetic field in Gyrotron, the electrons oscillate in their propagation path, while they rotate circular paths in Orbitron MASER.

A basic schematic view of Orbitron MASER is illustrated in figure 1(a). As depicted in this figure, it consists of an empty metallic cylinder with a metal wire (anode) in its center, and an electron emitter is closely located near the inner shell of the cylinder. The radii of cylinder and anode are indicated as R and R_0, respectively. As mentioned earlier, the strong radial electric field is created inside the cavity due to a high voltage applied between the anode at the tube center and the outer shell of the cavity. Therefore, some of the injected electrons are absorbed by anode which causes electric current flow; subsequently, the rest of electrons orbit around the anode. The orbiting electrons behave as negative mass particles, causing particle bunching due to their interaction with each other. This will leave them moving in different orbits around the anode and lead to the emission of electromagnetic radiation as a result of their acceleration [22].

Using the force balance between the attractive inward force of anode and the outward centrifugal force of electrons, the rotational frequency of particles can be obtained as [15, 22]:

$$\omega_0 = \frac{1}{r}\left(\frac{zeV}{m\ln\left(\frac{R}{R_0}\right)}\right)^{1/2} \tag{2.1}$$

where z, the sign and charge state of the particles, is set to -1 and e and m are electron charge and mass, respectively. Moreover, V is the voltage applied to the anode, and r, R, and R_0 respectively

2020 JINST 15 P01016

deonte the radii of an specific orbit, the cylinder, and the anode. According to eq. (2.1), the rotational frequency is dependent on the radius of the orbit, the radius of the cylinder and applied voltage to the anode, and can be tuned by the precise variation of these factors. However, increasing the applied voltage between the anode and the cathode (body) suffers from practical limitations in steady-state mode. Note that although Landau and Vlasov theory [20, 28] dictates the frequency of radiated waves must be roughly equal to the rotational frequency of particles, here the frequency of radiation is higher than the rotational frequency [15].

The radiation frequency due to the orbiting electrons is [15]:

$$\omega = \omega_0 \pm \left(\frac{1}{\sqrt{2}} + \frac{i}{\sqrt{2}}\right){\omega_0}^{3/2}\beta;$$

$$\beta = \frac{-Z_e e R n_e}{4\pi^2 V_r} \ln\left(\frac{r_2}{r_1}\right), \tag{2.2}$$

$$R = 2\pi r_{\text{ave}} \rho (l\Delta r)^{-1} \tag{2.3}$$

where radiation frequency is the real and positive part of ω, and R, r_{ave}, ρ, l, Δr, and n_e are resistance, the average radius of anode wire and cylinder, the resistivity of electron shell, cylinder length, the sum of anode wire and cylinder thicknesses and number of total electrons injected to the cylinder, respectively. As evident from the above equations, the emitted electromagnetic frequency is about ω_0. So, the calculated orbital angular frequency is in good agreement with simulation results.

One of the ways to increase the power of an orbitron MASER is to use multi-anode wires with the same voltages. Increasing the number of wires strengthens the radial electric field inside the structure much more compared to single-anode mode. In the former, the electrons will sense the radial periodic potentials because of anodes and they will accelerate more than the latter. Due to the strength of this static radial electric field, particles will gain more energy (resulting in more acceleration). If the phase locking occurs properly between the anode wires, the number of radiated coherent waves will be increased, which in turn will lead to higher output power and frequencies. In addition to manipulation of anode wires spacing, we have applied different voltages to anode wires in this paper to accelerate the electrons more than the condition with anodes of same voltages; increase in power radiation will be the result.

As stated above, enhancing the power of radiated waves in a single-frequency source can be achieved by the spatial arrangement of anodes and increasing the energy of injected electrons. The position of wires has to be arranged accurately in order to increase the apparent phase locking between the anodes and improve radiation power [20, 22]. In accordance with previous researches, power enhancement has been investigated in a multi-anode system with a constant voltage applied to the anodes.

Considering this idea, multiple-anode arrays in hexagonal arrangement with their specific applied potential differences has been proposed to improve the power efficiency. The schematic of proposed multi-anode Orbitron MASER has been illustrated in figure 1.b. As evident from this figure, the spacing and potential difference between the anodes are denoted by L and ΔV, respectively. The spatially-varying electric field inside the cavity can be created as a result of potential difference applied to the anodes. Consequently, the particles are accelerated in the orbits. Thus, the electrons orbiting around the anodes will have various energies in different places in the presence of spatially-varying electric field, leading to single-frequency and high power radiation.

2020 JINST 15 P01016

As illustrated in figure 1(b), the Orbitron MASER has six anodes in the center of a metallic cylinder in an elliptical pattern. As obvious, electrons in this multi-anodes pattern orbit in an oval shape and accelerate as the result of these anodes with different potentials. The electromagnetic radiation will be the outcome of this particle acceleration. The frequency of this radiation is $f_{6a} = \frac{v_0}{L}$, where v_0 is the average velocity of orbiting electron in the elliptical pattern, and L is the period of anodes [29]. As described earlier, $v_0 = r\omega_0$, so v_0 could be calculated from ω_0. Moreover, among the frequency components of electromagnetic radiation, the even ones are dominant in our obtained results.

3 Simulation results and discussions

As indicated former, the high power radiation in a single- and tunable-frequency source is desired in this work. To do this, multiple anodes has been utilized in a particular arrangement. Also, stable oscillation can be observed by increasing the initial energy of injected electrons inside the cavity. In this section, using CST particle studio software package that is dedicated to simulating the structure, microwave radiation in a single-anode and multi-anode Orbitron MASER have been examined through 3D simulation. Because the electromagnetic waves generated by charged particles acceleration inherently need both Maxwell equations and Lorentz forces, they have to be considered and solved simultaneously. Maxwell equations are required for electromagnetic wave computations and Lorentz forces govern the electric and magnetic forces applied to charge particles. As a result, the simulation method is based on 3D particle-in-cell (PIC) method, where Maxwell equations and Lorentz forces can be solved numerically and simultaneously. Simulation parameters are set as "Normal" for the background, "Open" for the boundary, and "Hexahedral" as the mesh type. Line per wavelength, cell around the edge, cells per max model box edge are respectively set to 20, 4 and 30 in the mesh settings, altogether corresponding to total 365,940 mesh cells.

We use a discrete voltage port between the cathode and anode in the CST-Particle studio to apply the anode voltage (1200 V). Regarding space charge, the emission model of electron source is "Explosive" with 60 particles located on the surface of electron source wire.

In the following, the output radiation of electromagnetic wave and the corresponding spectrum for the single-anode and multi-anode Orbitron MASERs are obtained. Additionally, the distribution of electric field and particles velocity in the proposed structure are investigated. Dependence of output power on the anodes spacing for various potential differences and cylinder radii is also studied.

The microwave radiation detected by a waveguide port which is located on the top and bottom of the cylinder is illustrated in figure 2(a) for single-anode Orbitron MASER. The radiated power can be calculated based on $P_{\text{abs}} = A_{\text{mp}}^2/2$, where A_{mp} is the amplitude of normalized output signal collected by waveguide port. The radii of cylinder and anode wire were chosen as 10 mm and 75 μm, respectively. In addition, the 1 KV voltage was applied between the anode wire and the outer shell of the cylinder (cathode), and the energy of injected electrons was set to 7 KeV.

As shown in figure 2(a), the stable oscillation can be observed after 150 ns at the output port. In figure 2(b), the FFT (Fast Fourier Transform) spectrum of the output radiation is calculated. According to this figure, the frequency of radiation is around 12.5 GHz. The output power of microwave radiation has been estimated as 3 kW when the energy of injected electrons was 7 KeV. By decreasing this energy, both the output power and frequency of radiation dropped, as shown in figure 3.

2020 JINST 15 P01016

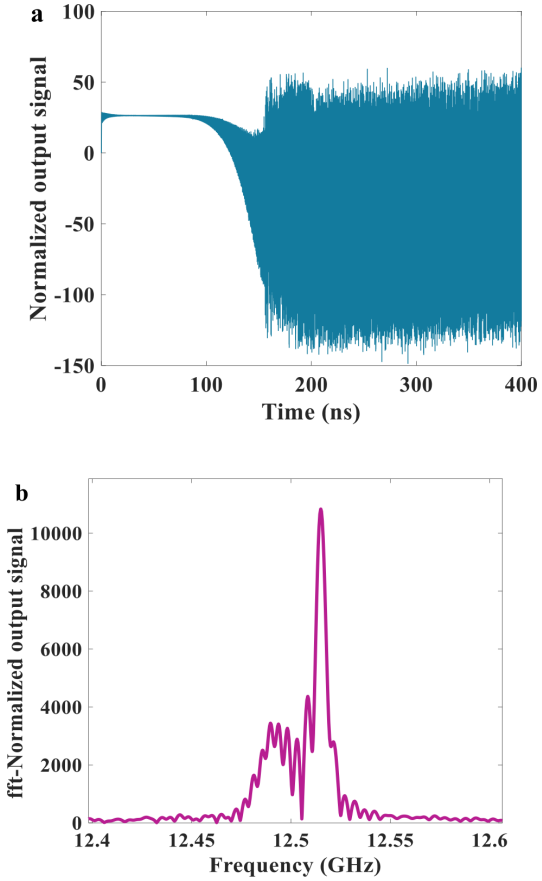

Figure 2. (a) Normalized output signal of single-anode Orbitron MASER when the applied initial energy of particles is 7 KeV. (b) Corresponding FFT of (a).

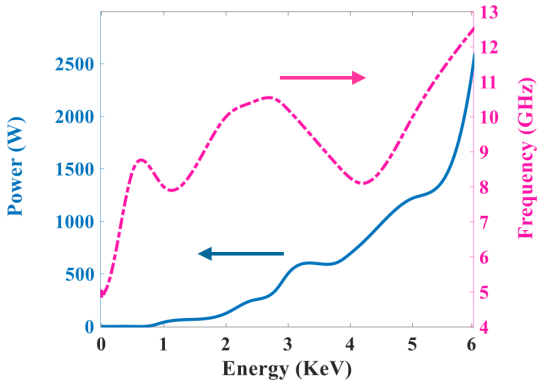

Figure 3. The dependence of output power (blue solid line) and output radiation frequency (pink dashed line) on the initial energy of electron emitter.

Output power, efficiency, and corresponding radiation frequency of single-anode Orbitron MASER have been measured experimentally as 10 μW, less than 0.01% and around 2 GHz, respectively [21]. Simulation results for this structure are well-conformed with the measured values. Contrary to prior works which had applied a hot filament for injecting electrons to the tube, we have

2020 JINST 15 P01016

Table 1. The parameters for Orbitron MASER.

The number of anodes	R [mm]	R_0 [μm]	Initial energy of electron [eV]	V [kV]	ΔV [V]	L [mm]
single-anode	10	75	150	1	—	—
3-anode in triangle arrangement	10	75	150	0.9	100	2
4-anode in square arrangement	10	75	150	0.6	200	2
6-anode in hexagonal arrangement	10	75	150	0.7	100	4

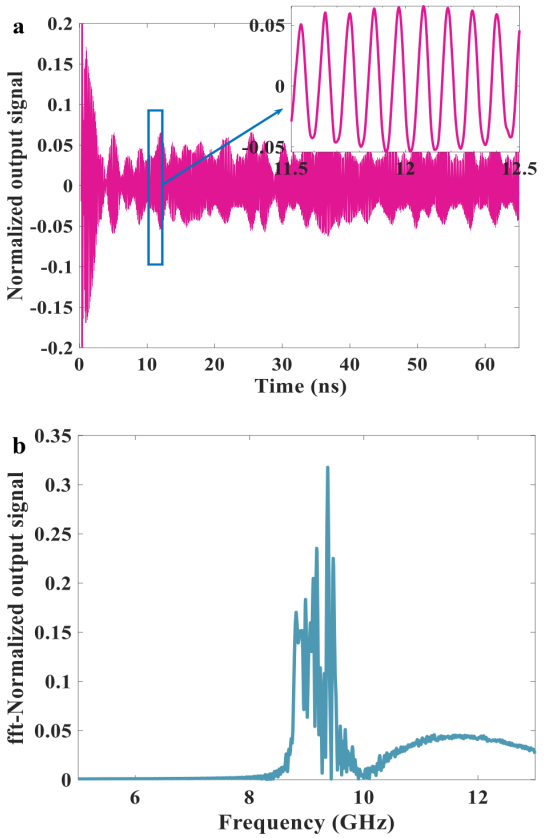

Figure 4. (a) Normalized output signal over time for single-anode Orbitron MASER when the initial energy of electrons is 150 V. The inset demonstrates some periods of the oscillation. (b) Corresponding FFT of (a). The parameters are listed in table 1.

used an electron emitter (like an electron gun) to this aim. The parameters of the single-anode Orbitron MASER are listed in table 1. The normalized output microwave signal collected by waveguide port and its corresponding FFT spectrum are depicted in figures 4(a) and 4(b), respectively. As one can see in table 2, the calculated output power is about 3.2 mW, and the efficiency is 0.003%.

Previously stated in this paper, the output power has been enhanced by increasing the number of anodes in a unique arrangement at cavity center. To do this, 3-anode Orbitron MASER has been proposed in which the anodes are located at cylinder center as the vertices of a triangle. The anodes spacing is $L = 2$ mm and the initial voltage applied to the anode is 900 V; the voltage difference between the anodes is set to 100 V (i.e., the voltage of anodes are 900 V, 1000 V, and 1100 V). In this case, the output power of 15 mW with 0.004% efficiency has been observed with an oscillation frequency equal to 10.55 GHz.

2020 JINST 15 P01016

Table 2. Characteristics of electromagnetic radiation for Orbitron MASER.

Number of anodes	Frequency of radiation [GHz]	Output power [mW]	Efficiency %
simulation of single-anode [9]	>2	0.01	0.002
single-anode	9.2	3.2	0.003
3-anode in triangle arrangement	10.55	15	0.004
4-anode in square arrangement	10	15	0.0045
6-anode in hexagonal arrangement	7.9	180	> 0.01

By locating 4 anodes in the vertices of a 2 mm × 2 mm square at cavity center and applying an initial voltage equal to 600 V with 200 V potential difference between the anodes, the output power and the frequency of radiation were obtained the same as 3-anode Orbitron MASER, and the efficiency was about 0.0045%. Structural parameters and the simulation results for each case are listed in tables 1 and 2, respectively.

Figure 1(b) represents that 6 anodes are located at the vertices of a hexagon to enhance the output radiation power. The anodes spacing, initial voltage of anodes and their potential difference are respectively 4 mm, 700V, and 100V, as listed in table 1. The output microwave radiation of 6-anode Orbitron MASER and its FFT spectrum have been illustrated in figures 5(a) and 5(b), respectively. Wave-particle power transfer (power transfer between electrons and electromagnetic waves) for 6-anode Orbitron MASER has been depicted in figure 5(c) with its spectrum shown in figure 5(d). This power transfer has some peaks same as the output radiations. A single-frequency oscillation has been observed at 7.9 GHz. Also, the output power and efficiency have been calculated as almost 180 mW and > 0.015% respectively, which are much higher than the previous studies.

In summary, figure 6 exhibits the spectrum of output radiation for single- anode, 3-anode, 4-anode, and 6-anode Orbitron MASERs. The electric field distribution inside the cavity for the single-anode and 6-anode Orbitron MASERs are shown in figure 7(a) and b, where the energy of injected electrons is 150 eV. Figure 7 depicts the electrical distribution of anodes with its maximum around the anodes.

As described, the injected electrons inside the cavity are orbiting around the anode wires in different orbits as a result of NMI theory. As in figure 8(a), the electron bunch is rotated around the anode in a single-anode Orbitron MASER at t = 10, 60 and 70 ns, where the population inversion happens naturally [19]. Besides, the rotation of electrons in 6-anode Orbitron MASER has been depicted in figure 8(b) for different values of t = 2.4, 3, and 10 ns. It is clearly seen in figure 8 that the phase locking intensifies significantly when the number of anodes is increased, and the particles rotate in bunches around the anode wires. The apparent phase locking around the anode of the highest voltage is also increased in 6-anode Orbitron MASER, leading to enhancement of output power. Accordingly, the position and the voltage applied to the anodes are the most critical parameters for radiation power improvement [15, 22].

Furthermore, the velocity distribution of particles (β), defined as particle velocity per speed of light has been shown in figures 9(a) and 9(b) for single-anode and 6-anode Orbitron MASERs, respectively. The distribution of β for the particles in a single-anode structure has been estimated around 0.01 to 0.02 (the distribution of particle velocity is about 3×10^6 to 6×10^6 m/s), and the number of particles with lower speeds is much more than those with high speeds, as seen in

2020 JINST 15 P01016

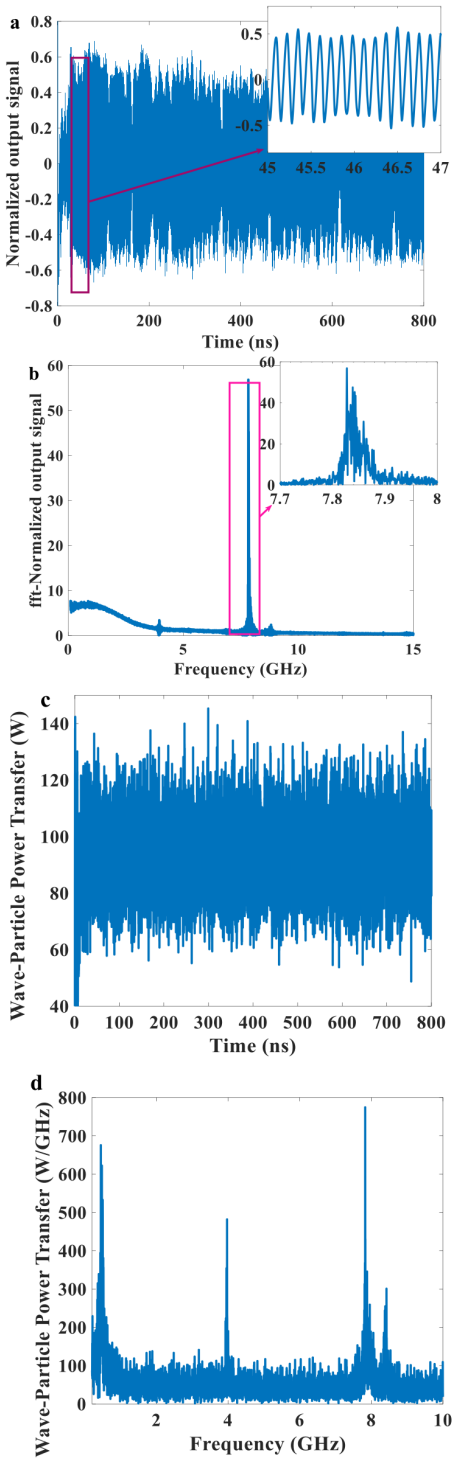

Figure 5. (a) Normalized output signal of 6-anode Orbitron MASER when the potential difference between the anodes is 100 V. The inset demonstrates some periods of oscillation. (b) Corresponding FFT of (a). (c) wave-particle power transfer and (d) frequency spectrum of (c). The structural parameters are listed in table 1.

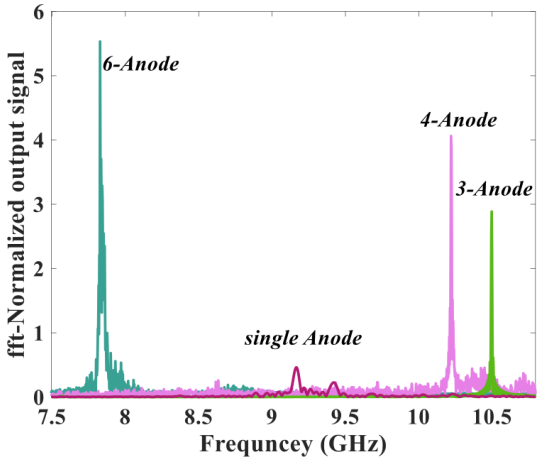

Figure 6. The FFT spectrum of normalized output signal for single-anode, 3-anode in triangle arrangement, 4-anode in square method and 6-anode in hexagonal arrangement Orbitron MASERs (6-anode amplitude decreases ten times).

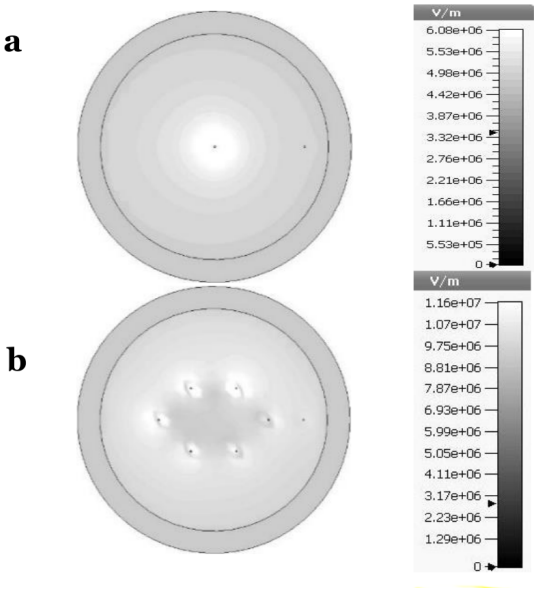

Figure 7. Electric field distribution inside (a) single-anode (b) 6-anode Orbitron MASERs in hexagonal arrangement.

figure 9(a). Spatially-varying electric field distribution inside the cavity is created as a result of potential difference applied to the anodes in a particular position, causing the particles to accelerate in orbits. Thus, the single frequency and high power radiation can be observed due to particles velocity increase. The distribution of β for 6-anode Orbitron MASER spans 0.01 to 0.06 interval, equivalent to the velocity of 3×10^6 to 1.8×10^7 m/s. Comparing this figure with figure 9(a) reveals that in addition to doubling the particle velocity, particle number distribution at various speeds, especially at high values is very high. As shown in figure 9(b), phase bunching for 6-anode Orbitron MASER occurs eight times along the tube at t = 6 ns. This phase bunching results in the radiation

2020 JINST 15 P01016

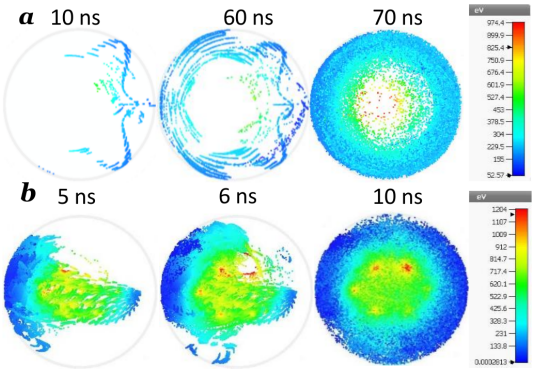

Figure 8. The distribution and orbiting of electrons for (a) single-anode and (b) 6-anode Orbitron MASERs.

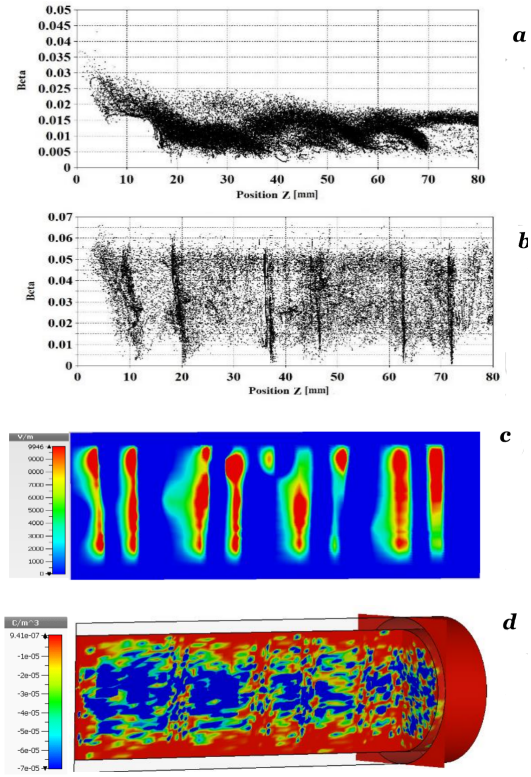

Figure 9. The distribution of Beta for (a) single-anode, (b) 6-anode Orbitron MASERs at t = 6 ns, (c) electrical field distribution for 6-anode Orbitron MASER at t=6ns with 7.82 GHz frequency, and (d) distribution of space charge in 6 anodes by max of 0.0002 C/m^3 and min of 0.002 C/m^3.

of electromagnetic waves, as with figure 9(c). Figure 9(c) illustrates that electromagnetic radiations occur proportional to 8-line phase bunching of electrons for 6-anode Orbitron MASER.

The oscillation output power and frequency can be enhanced as a result of particles velocity increase so as to engineer the electric field distribution inside the cavity. With this in mind, arrangement and applied voltages to the anodes have to be chosen appropriately to control the field distribution around the anode wires. In this direction, the dependence of radiation output power and

2020 JINST 15 P01016

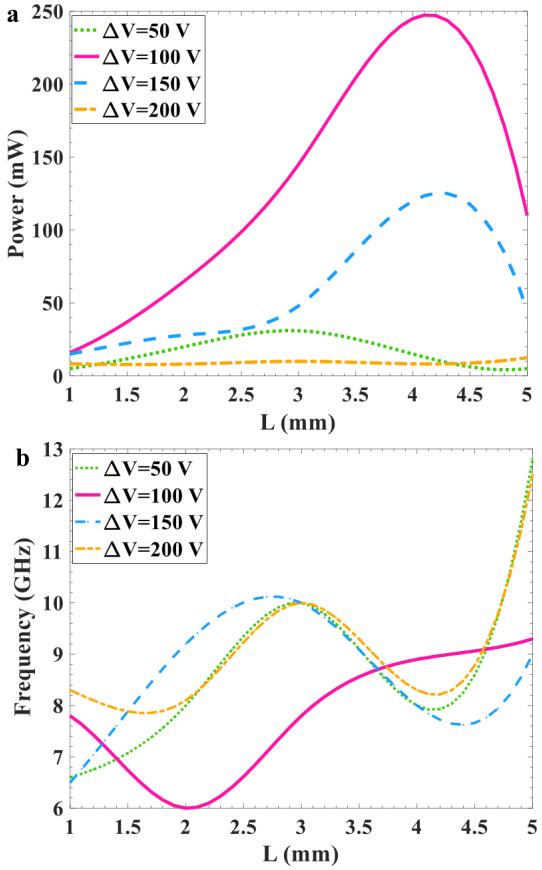

Figure 10. The dependence of (a) output power and (b) output radiation frequency on anodes spacing for various applied potential differences between the anodes.

frequency on the anodes spacing and their potential difference in 6-anode Orbitron MASER have been examined and depicted in figures 10(a) and 10(b), respectively. It is apparent from figure 9(a) that for $\Delta V = 100\,\mathrm{V}$ and $L = 4\,\mathrm{mm}$, the maximum value of almost 180mW can be achieved for output power with an efficiency more than 0.015%. Also, the corresponding radiation frequency is nearly 8 GHz.

Finally, the variation of cylinder radius has been studied for the optimal value of L and ΔV. Based on eq. (2.1), the frequency of oscillation is slightly increased and the output power is enhanced by decreasing the cylinder size. Figure 11 displays the effect of cylinder radius increase for the optimum structure. This increase does not significantly impact the efficiency, frequency, and output power.

4 Conclusion

In this paper, the improvement of oscillation output power and frequency for the Orbitron MASER have been investigated. To do this, the number of anodes and their arrangement have been modified to enhance the particles velocity and increase the phase locking between them by engineering the electric field distribution. By changing the position of anodes and the applied voltage, the velocity of particle bunches inside the cavity rises to 2×10^7 m/s. Subsequently, the microwave radiation

2020 JINST 15 P01016

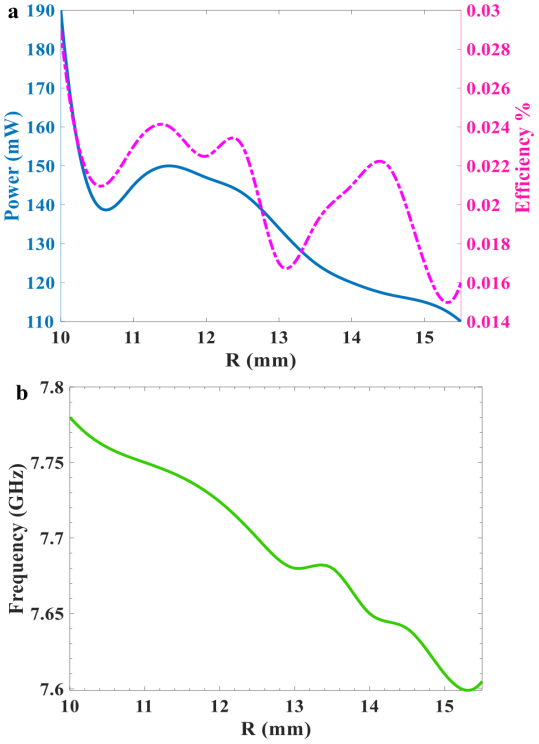

Figure 11. The dependence of (a) output power and efficiency and (b) the output radiation frequency on cylinder radius.

has been observed in single-frequency source with an oscillation frequency improvement from 2 GHz to 8 GHz; besides, the radiation output power has been enhanced to 185 mW in 6-anode Orbitron MASER.

Acknowledgments

There is no conflict of interest.

References

[1] S. Kharkovsky and R. Zoughi, *Microwave and millimeter wave nondestructive testing and evaluation — Overview and recent advances*, *IEEE Instrum. Meas. Mag.* **10** (2007) 26.

[2] J.B. Jarvis et al., *Analysis pf an open-ended coaxial probe with lift off for nondestructive testing*, *IEEE Trans. Instrum. Meas.* **43** (1994) 711.

[3] J. Hasch et al., *Millimeter-wave technology for automotive radar sensors in the 77 GHz frequency band*, *IEEE Trans. Microw. Theor. Techn.* **60** (2012) 845.

[4] W.C. Brown and E.E. Eves, *Beamed microwave power transmission and its application to space*, *IEEE Trans. Microw. Theor. Techn.* **40** (1992) 1239.

[5] T. Chen, S. Li and H. Sun, *Metamaterials application in sensing*, *Sensors* **12** (2012) 2742.

[6] T. Nitsche et al., *IEEE 802.11ad: directional 60 GHz communication for multi-Gigabit-per-second Wi-Fi*, *IEEE Commun. Mag.* **52** (2014) 132.

2020 JINST 15 P01016

[7] V. Jaeck et al., *A conical patch antenna array for agile point-to-point communications in the 5.2 GHz band*, *IEEE Antennas Wireless Propag. Lett.* **15** (2015) 1230.

[8] X. Chen and D. Li, *High power Terahertz generation by using vacuum electronic technology*, in the proceedings of the 2nd *IEEE International Conference on Broadband Network Multimedia Technology*, October 18–20, Beijing, China (2009).

[9] A. Shukla, M. Saxena and K.V. Pandey, *A brief review on operation of gyrotron — A microwave device*, *Int. Res. J. Engineer. Technol.* **2** (2015) 307.

[10] A. Shukla et al., *Introduction of gyrotron as fast wave device*, *MIT Int. J. Electron. Commun. Engineer.* **3** (2013) 94.

[11] S.H. Gold and G.S. Nusinovich, *Review of high-power microwave source research*, *Rev. Sci. Instrum.* **68** (1997) 3945.

[12] M.G. Nimmura et al., *A prototype commercial orbitron maser for milimeterwave rader*, in the proceedings of the 13th *International Conference on Infrared and Millimeter Waves*, December 5–8, Honolulu, U.S.A. (1987).

[13] D.M. French et al., *Causes of efficiency roll-off in phosphorescent organic light emitting devices: Triplet-triplet annihilation versus triplet-polaron quenching*, *Appl. Phys. Lett.* **97** (2010) 11501.

[14] V.Y. Kirichenko, *Phase selection of electrons in Orbitron-type systems*, *Radioelectron. Commun. Syst.* **49** (2006) 9.

[15] I. Alexeff and F. Dyer, *Millimeter microwave emission from a maser by use of plasma-produced elecrons orbiting a positively charged wire*, *Phys. Rev. Lett.* **45** (1980) 351 [*Erratum ibid.* **45** (1980) 764].

[16] I. Alexeff, F. Dyer and W. Nakonieczny, *Leaky characteristics of a new millimeter wave antenna based on groove guide with an asymmetric conductor strip*, *Int. J. Infrared Millimeter Waves* **6** (1985) 481.

[17] I. Alexeff, F. Dyer and M. Rader, *Pulsed and steady-state multinode orbitron masers*, in the proceedings of the 13th *International Conference on Infrared and Millimeter Waves*, December 5–8, Honolulu, U.S.A. (1987).

[18] I. Alexeff, M. Radar and F. Dyer, *Recent developments in the Orbitron maser*, in the proceedings of the 20th *Southeastern Symposium on System Theory*, March 20–22, Knoxville, U.S.A. (1988).

[19] M. Rader, I. Alexeff and F. Dyer, *Steady-state orbitron emissions*, *IEEE Trans. Plasma Sci.* **15** (1987) 56.

[20] I. Alexeff, *A simplified Vlasov-Landau treatment of electron motion in the orbitron maser*, *Phys. Fluids* **28** (1980) 1990.

[21] I. Alexeff, F. Dyer and M. Rader, *Recent results on the Orbitron maser*, *Nucl. Instrum. Meth.* **A 285** (1989) 228.

[22] M. Rader, *Development of the high vacuum steady-state*, M.Sc. thesis, University of Tennessee, Knoxville, U.S.A. (1980).

[23] J.M. Burke, W.M. Manheimer and E. Ott, *Theory of the orbitron maser*, *Phys. Rev. Lett.* **56** (1986) 2625.

[24] V.M. Gul'kon et al., *Characteristics of an "orbitron" ion source with a two-wire anode*, *Russ. Phys. J.* **34** (1991) 977.

[25] G.W. McClure, *Low-pressure glow discharge*, *Appl. Phys. Lett.* **2** (1963) 233.

2020 JINST 15 P01016

[26] M. Makarov and Y. Loumani, *Pulsed low-pressure wire discharge*, *J. Appl. Phys.* **100** (2006) 033301.

[27] I. Alexeff et al., *Negative mass instability in low voltage Cyclotron Resonance Maser*, in the proceedings of the *International Conference on Mathematical Methods in Electromagnetic Theory*, August 28–30, Kyiv, Ukraine (2012).

[28] J.M. Burke, *Negative mass instability in low voltage Cyclotron Resonance Maser*, *Phys. Fluids* **B 3** (1991) 471.

[29] S.A. Mikhailov, *Graphene-based voltage-tunable coherent TeraHertz emitter*, *Phys. Rev.* **B 87** (2013) 115405.

[30] *CST — Computer Simulation Technology*, https://www.cst.com.

2020 JINST 15 P01016